

1-2018

Role of Acid-Sensing Ion Channels in Hypoxia- and Hypercapnia-Induced Ventilatory Responses

Neil D. Detweiler

University of New Mexico Health Sciences Center, ndetweiler@salud.unm.edu

Kenneth Vigil

University of New Mexico, Kennethv7@unm.edu

Thomas C. Resta

University of New Mexico Health Sciences Center, tresta@salud.unm.edu

Benjimen R. Walker

University of New Mexico Health Sciences Center, bwalker@salud.unm.edu

Nikki L. Jernigan

Follow this and additional works at: https://digitalrepository.unm.edu/cell_pubs



Part of the [Medicine and Health Sciences Commons](#)

Recommended Citation

Detweiler, Neil D.; Kenneth Vigil; Thomas C. Resta; Benjimen R. Walker; and Nikki L. Jernigan. "Role of Acid-Sensing Ion Channels in Hypoxia- and Hypercapnia-Induced Ventilatory Responses." *Role of Acid-Sensing Ion Channels in Hypoxia- and Hypercapnia-Induced Ventilatory Responses* (2018). https://digitalrepository.unm.edu/cell_pubs/4

This Article is brought to you for free and open access by the Cell Biology and Physiology at UNM Digital Repository. It has been accepted for inclusion in Cell Biology and Physiology Research and Scholarship by an authorized administrator of UNM Digital Repository. For more information, please contact disc@unm.edu.

1 **Role of Acid-Sensing Ion Channels in Hypoxia- and Hypercapnia-Induced**
2 **Ventilatory Responses**

3
4 Neil D. Detweiler, Kenneth G. Vigil, Thomas C. Resta, Benjimen R. Walker, and Nikki L.
5 Jernigan
6

7 Short title: Role of Acid-Sensing Ion Channels in Regulation of Breathing
8
9
10

11
12 Affiliation for all authors:

13 Vascular Physiology Group
14 Department of Cell Biology and Physiology
15 University of New Mexico Health Sciences Center
16 Albuquerque, NM, USA
17

18 Corresponding author contact information:

19 Nikki L. Jernigan, Ph.D.
20 Department of Cell Biology and Physiology
21 University of New Mexico Health Sciences Center
22 1 University of New Mexico
23 MSC08-4750
24 Albuquerque, NM 87131
25 NJernigan@salud.unm.edu
26

27 **Abstract:**

28 Previous reports indicate roles for acid-sensing ion channels (ASICs) in both
29 peripheral and central chemoreception, but the contributions of ASICs to ventilatory
30 drive in conscious, unrestrained animals remain largely unknown. We tested the
31 hypotheses that ASICs contribute to hypoxic- and hypercapnic-ventilatory responses.
32 Blood samples taken from conscious, unrestrained mice chronically instrumented with
33 femoral artery catheters were used to assess arterial O₂, CO₂, and pH levels during
34 exposure to inspired gas mixtures designed to cause isocapnic hypoxemia or
35 hypercapnia. Whole-body plethysmography was used to monitor ventilatory parameters
36 in conscious, unrestrained ASIC1, ASIC2, or ASIC3 knockout (^{-/-}) and wild-type (WT)
37 mice at baseline, during isocapnic hypoxemia and during hypercapnia. Hypercapnia
38 increased respiratory frequency, tidal volume, and minute ventilation in all groups of
39 mice, but there were no differences between ASIC1^{-/-}, ASIC2^{-/-}, or ASIC3^{-/-} and WT.
40 Isocapnic hypoxemia also increased respiratory frequency, tidal volume, and minute
41 ventilation in all groups of mice. Minute ventilation in ASIC2^{-/-} mice during isocapnic
42 hypoxemia was significantly lower compared to WT, but there were no differences in the
43 responses to isocapnic hypoxemia between ASIC1^{-/-} or ASIC3^{-/-} compared to WT.
44 Surprisingly, these findings show that loss of individual ASIC subunits does not
45 substantially alter hypercapnic or hypoxic ventilatory responses.

46 **Introduction:**

47 Arterial O₂, CO₂, and pH (P_aO₂, P_aCO₂, and pH_a) homeostasis is maintained by
48 reflex control of ventilation. Alterations in P_aO₂, P_aCO₂, and pH_a are detected by
49 peripheral chemoreceptors located in type I glomus cells within the carotid and aortic
50 bodies. P_aCO₂ homeostasis is additionally regulated by central chemoreceptors located
51 on the ventral surface of the medulla as well as other brain regions (1). Activation of
52 carotid chemoreceptors in response to hypoxemia, hypercapnia, or acidosis leads to
53 inhibition of K⁺ channels, depolarization of the chemoreceptor cells, activation of L-type
54 Ca²⁺ channels, and release of excitatory neurotransmitters that subsequently stimulate
55 ventilation and sympathetic activation (2–8). Although this model of carotid body
56 chemoreception is generally accepted, there are several O₂- and CO₂/pH-sensitive ion
57 channels and other proteins and their individual and integrated roles in chemoreception
58 remain incompletely understood. The precise location of *central* chemoreception also
59 remains uncertain, and it appears that several brain regions are involved (1). A major
60 mechanism by which central chemoreceptors detect CO₂ levels is thought to be the
61 detection of secondary changes in cerebrospinal fluid pH (1). Ion channels are generally
62 the favored candidates for central chemoreception (9), but the identity of the specific
63 channels involved remains unclear, with several candidates having been proposed (10–
64 13). One family of ion channels implicated in both peripheral and central
65 chemoreception is that of the proton-gated, acid-sensing ion channels (ASICs).

66 ASICs are members of the degenerin\epithelial Na⁺ channel (DEG/ENaC)
67 superfamily that form trimeric cation channels. ASIC genes (ASIC1-4) and their splice
68 variants (ASIC1a, -1b, -2a, -2b, -3, and -4) form homo- or hetero-multimeric channels

69 with different pH sensitivities. ASIC1 and 3 homomers are the most sensitive to acidic
70 conditions with a half-maximal activation (pH_{50}) of around pH 6.5 (14,15); whereas
71 ASIC2 is least acid-sensitive ($\text{pH}_{50} \sim 4.9$) (15). ASIC1 and 3, and to a lesser extent
72 ASIC2, are expressed in glomus cells and the transient acid-evoked depolarization of
73 isolated glomus cells is consistent with the biophysical and pharmacological properties
74 of ASICs (16). ASICs are also widely expressed in the medulla where reductions in pH
75 trigger ASIC-like currents and stimulation of phrenic nerve activity in anesthetized
76 animals (17–19). Based on these reports that suggest that ASICs play an important role
77 in chemoreception, we hypothesized that ASICs contribute to hypercapnic/acidosis-
78 induced ventilatory drive in conscious, unrestrained mice.

79 Recent studies from our laboratory also demonstrate that ASIC1, expressed in
80 pulmonary arterial smooth muscle cells (PASMC), contributes to hypoxic pulmonary
81 vasoconstriction (HPV) (20). Although the precise mechanism remains unclear, HPV is
82 generally thought to be an intrinsic response of O_2 -sensing PASMC, supporting
83 ventilation-perfusion matching for optimal gas exchange in the lung by diverting blood
84 flow away from hypoxic regions of the lung. Our data showing reduced HPV in ASIC1
85 null mice (20) suggest ASICs are sensitive to changes in O_2 . Therefore, we further
86 hypothesized that ASICs additionally contribute to the *hypoxic* ventilatory response. To
87 test our hypotheses, we examined ventilatory responses to isocapnic hypoxemia and
88 hypercapnia in conscious, unrestrained, ASIC1, 2, or 3 global knockout (ASIC1^{-/-}, 2^{-/-}, or
89 3^{-/-}) and wild-type (WT) mice.

90 **Materials and Methods:**

91 Animals

92 All protocols used in this study were reviewed and approved by the Institutional
93 Animal Care and Use Committee of the University of New Mexico School of Medicine
94 (Protocol number: 16-200543-HSC) and abide by the National Institutes of Health
95 guidelines for animal use. All surgeries (described below) were performed under
96 isoflurane anesthesia and buprenorphine was used for post-operative analgesia. ASIC1
97 (B6.129-Asic1^{tm1Wsh/J}), ASIC2 (B6.129-Asic2^{tm1Wsh/J}), and ASIC3 (B6.129-Asic3^{tm1Wsh/J})
98 knockout (^{-/-}) mice (all from Jackson Laboratory, Bar Harbor, ME) were bred on a
99 C57BL/6 background and compared to age-matched C57BL/6 wildtype (WT) controls.
100 Disruption of the relevant ASIC was confirmed by PCR and agarose gel electrophoresis
101 using a three-primer (ASIC1^{-/-} and ASIC2^{-/-}) or four-primer (ASIC3^{-/-}) system to detect
102 both WT and disrupted alleles. The following primers were used for genotyping: ASIC1:
103 5'-CAT GTC ACC AAG CTC GAC GAG GTG-3' (WT forward primer), 5'-TGG ATG TGG
104 AAT GTG TGC GA-3' (knockout forward primer), 5'-CCG CCT TGA GCGGCA GGT
105 TTA AAG G-3' (reverse primer); ASIC2: 5'-AGT CCT GCA CGG TGG GAG CTT CTA-3'
106 (reverse primer) 5'-GAA GAG GAA GGG AGC CAT GAT GAG-3' (WT forward primer),
107 5'-TGG ATG TGG AAT GTG TGC GA-3' (knockout forward primer); ASIC3: 5'-GAA
108 CCT GGA AAA CAG AGG CAG GAA GGA T-3' (knockout reverse primer), 5'-CAG
109 GGA GTA AGA TCT TAT GTA GCC TGG C-3' (knockout forward primer), 5'-TGG ATG
110 TGG AAT GTG TGC GA-3' (WT reverse primer), 5'-CCC TGG GCA CCA GAG TTG
111 AAG GTG TAG C-3' (WT forward primer). Males and females (~15 wk old) were used

112 equally. Each group of knockout mice was paired with a separate, simultaneously run
113 set of WT mice.

114

115 Femoral artery catheterization and blood gas measurement

116 To confirm that alterations in inspired gases were achieving the desired effect on
117 blood gases, and that blood gases were similar between paired groups of WT and
118 knockouts, mice were chronically instrumented with femoral artery catheters for arterial
119 blood sampling to determine P_{aO_2} , P_{aCO_2} , and pH_a . The catheters were routed out
120 through the top of the cage through spring tethers to enable blood sampling in
121 conscious, unrestrained mice. Catheters consisted of PE-10 tubing with a stretch-
122 tapered proximal end for insertion into the right femoral artery, and were filled with a
123 solution of 0.9% saline containing 100 units/ml heparin. Catheterization was performed
124 under isoflurane anesthesia (5% isoflurane for induction of anesthesia, ~2% for
125 maintenance) and mice were given buprenorphine (0.05 – 0.1 mg/kg, s.c.) and
126 enrofloxacin (15 mg/kg, s.c.) post-operatively for analgesia and protection from
127 infection, respectively.

128 Blood gas measurements were performed 2 days after the implantation surgery.
129 For these experiments, mice were placed in a polycarbonate chamber for exposure to
130 different inspired gas mixtures. A Columbus Instruments PEGAS 4000MF gas mixer
131 (Columbus, OH) was used to combine N_2 , O_2 , and CO_2 for the appropriate inspired gas
132 mixtures, the compositions of which were confirmed using an OxiGraf O_2 Cap Oxygen
133 [and CO_2] Analyzer (Sunnyvale, CA) to test samples taken from chamber inflow line. To
134 measure blood gases, ~100 μ L of blood was allowed to flow directly from the femoral

135 artery catheter into Abbott iStat handheld blood gas analyzer cartridges (EG6+ or G3+,
136 Abbott Park, IL) while the mouse was conscious and unrestrained. Each measurement
137 was taken after 5 minutes of exposure to the respective inspired gas mixture, with at
138 least 20 minutes between subsequent exposures. The catheter was flushed with a
139 volume of saline (containing 100 units/mL heparin) equivalent to 1.5 times the dead
140 space of the catheter between each measurement. For each individual mouse, all blood
141 gas measurements were performed on a single day.

142

143 Whole-body Plethysmography

144 Whole-body plethysmography was used to assess respiratory frequency, tidal
145 volume, and minute ventilation in conscious, unrestrained mice. First described by
146 Drorbaugh and Fenn (21), this method utilizes a nearly sealed chamber in which the
147 pressure transiently increases as inspired air expands due to the humidity and warmth
148 of the lung compared to the surrounding environment. For this study we modified a
149 method previously used for rats (22). The plethysmography chamber consisted of a ~50
150 cubic centimeter transparent polycarbonate cylinder fitted with a Validyne DP45-16
151 differential pressure transducer and inlets for the introduction of new inspired gas
152 mixtures. To take a measurement, the chamber was sealed with the exception of a
153 small controlled leak through a 50 μ l glass syringe (Gastight #1705) with plunger
154 removed, attached to one of the Luer-lock ports on the side of the chamber, which
155 served as a physical high-pass filter to eliminate gradual changes in chamber pressure
156 that go beyond the narrow range of the highly sensitive differential pressure transducer.
157 Temperature inside the chamber was monitored using an electronic probe (BAT-10,

158 Physitemp, Clifton, NJ) and ranged from 21 to 25° C. Calibration air injections of 40 µl
159 were used to enable calculation of tidal volume using the equation introduced by
160 Drorbaugh and Fenn (21):

161

$$162 \quad V_T = \frac{P_T}{P_K} \times V_K \times \frac{T_R(P_B - P_C)}{T_R(P_B - P_C) - T_C(P_B - P_R)}$$

163 Where:

164 V_T = tidal volume

165 V_K = the volume of air injected into the animal chamber for calibration

166 P_T = the pressure deflection associated with each tidal volume

167 P_K = the pressure deflection associated with injection of the calibrating volume, V_K

168 T_R = body temperature, assumed to be 37 °C for all animals

169 T_C = the air temperature in the chamber, which varied from 20-23 °C

170 P_B = barometric pressure, 630 mmHg in Albuquerque, NM

171 P_R = vapor pressure of water at body temperature

172 P_C = vapor pressure of water in the chamber, derived from T_C assuming 100% humidity

173 which was confirmed in pilot experiments (gas mixtures were humidified by

174 bubbling through three consecutive flasks of water prior to entry into the

175 plethysmography chamber)

176

177 Tidal volume and minute ventilation data were normalized to body mass. The

178 plethysmography chamber was never closed from gas flow for measurement for more

179 than 2 consecutive minutes, and the chamber was continuously flushed with fresh gas

180 mixture for at least 2 minutes between measurements at a flow rate of 2 L/min. Mice

181 were allowed up to 1 hour to achieve a resting state suitable for baseline measurements
182 (lack of movement, grooming, or sniffing as observed through the transparent walls of
183 the chamber). Mice that remained active after 1 hour were removed from the chamber
184 and re-tested on another day. After a baseline measurement was taken, the chamber
185 was flushed with 21% O₂, 6% CO₂, balance N₂ to achieve hypercapnia, or 7% O₂, 3.2%
186 CO₂, balance N₂ to achieve isocapnic hypoxemia for 5 minutes before taking the
187 subsequent measurement.

188

189 Statistics

190 All data are expressed as means \pm SE. n values correspond to the numbers of
191 animals per group. Statistical tests are specified in the figure legends or in the results
192 section, and were made using GraphPad Prism 7.02 software (La Jolla, CA). *P* values
193 of <0.05 were accepted as significant for all comparisons.

194

195 **Results**

196 Examining the roles of ASIC1, 2, and 3 in the hypercapnic ventilatory response

197 To investigate the roles of ASIC1, 2, and 3 in the hypercapnic ventilatory
198 response, we first assessed changes in ventilation during exposure to increasing levels
199 of inspired CO₂ (3.7, 6.0, and 9.8%) using whole-body plethysmography in conscious,
200 unrestrained WT mice. The traces shown in Fig. 1A represent the pressure difference
201 between the inside and the outside (room pressure) of the chamber. Upward pressure
202 deflections indicate increasing pressure in the animal chamber (inspiration). The
203 amplitude of the pressure deflections corresponds to tidal volume. Respiratory
204 frequency (Fig 1B, breaths/min) was determined by counting the number of pressure
205 deflections per minute. Exact tidal volume normalized to body mass (Fig 1C,
206 $\mu\text{L}/\text{breath}/\text{g}$) was calculated using chamber temperature and calibration air injection
207 (see Methods). Minute ventilation normalized to body mass (Fig 1D, $\text{mL}/\text{minute}/\text{gram}$)
208 was determined by multiplying tidal volume by respiratory frequency.

209

210 Figure 1 caption:

211 **Inhalation of 6% CO₂ produces reliable hypercapnia and elevation of**
212 **ventilation.** WT mice were exposed to a range of inspired CO₂ levels to
213 determine optimal conditions for testing hypercapnic ventilatory responses. **(A)**
214 Representative traces of whole-body plethysmography illustrate frequency and
215 depth of breathing in conscious, unrestrained mice exposed to normal air at
216 baseline (21% O₂, 0% CO₂, balance N₂), and to increasing levels of hypercapnia
217 (3.7, 6.0, and 9.8% CO₂). Summary data shows **(B)** respiratory frequency

218 (breaths/min), **(C)** tidal volume ($\mu\text{L}/\text{breath}/\text{g}$), and **(D)** minute ventilation
219 ($\text{mL}/\text{min}/\text{g}$) at each inspired CO_2 level. Arterial blood samples taken from WT
220 mice at baseline (normal air) or during exposure to 6% CO_2 were analyzed for **(E)**
221 P_aO_2 , **(F)** P_aCO_2 , and **(G)** pH_a . Values are means \pm SE; $n = 4-8$ animals/group. * P
222 < 0.05 vs. baseline (1-way ANOVA; Dunnett's post-hoc test (B) or two-tailed,
223 paired Student's t-test (C-E)).

224 **Table 1 – Blood gas levels were not different between paired WT and knockout**
 225 **groups at baseline, during hypercapnia, or during isocapnic hypoxemia.**

Baseline (21% O₂, 0% CO₂, balance N₂)						
	WT	ASIC1 ^{-/-}	WT	ASIC2 ^{-/-}	WT	ASIC3 ^{-/-}
P _a O ₂	63.2 ± 0.9	66.4 ± 0.8	58.6 ± 1.0	62.1 ± 2.2	64.9 ± 0.9	70.9 ± 2.7
P _a CO ₂	28.0 ± 1.1	26.2 ± 0.5	28.4 ± 0.3	29.3 ± 1.0	27.4 ± 0.8	26.7 ± 1.2
pH _a	7.37 ± 0.01	7.39 ± 0.01	7.38 ± 0.01	7.39 ± 0.01	7.36 ± 0.01	7.34 ± 0.02
Hypercapnia (21% O₂, 6.0% CO₂, balance N₂)						
	WT	ASIC1 ^{-/-}	WT	ASIC2 ^{-/-}	WT	ASIC3 ^{-/-}
P _a O ₂	100.2 ± 2.1*	99.6 ± 2.1*	90.3 ± 1.2*	95.9 ± 2.9*	100.1 ± 1.4*	103.6 ± 3.5*
P _a CO ₂	45.9 ± 1.5*	45.8 ± 0.8*	44.8 ± 0.7*	45.5 ± 0.9*	47.9 ± 0.9*	45.8 ± 0.9*
pH _a	7.23 ± 0.02*	7.22 ± 0.01*	7.23 ± 0.01*	7.24 ± 0.02*	7.21 ± 0.01*	7.20 ± 0.02*
Isocapnic hypoxemia (7.0% O₂, 3.2% CO₂, balance N₂)						
	WT	ASIC1 ^{-/-}	WT	ASIC2 ^{-/-}	WT	ASIC3 ^{-/-}
P _a O ₂	40.3 ± 1.5*	40.4 ± 0.6*	35.6 ± 1.2*	38.5 ± 1.4*	39.3 ± 0.8*	42.7 ± 1.5*
P _a CO ₂	25.5 ± 0.8*	25.1 ± 0.5	25.6 ± 0.4*	26.1 ± 0.7*	28.0 ± 0.6	27.3 ± 0.6
pH _a	7.39 ± 0.02	7.39 ± 0.00	7.40 ± 0.01	7.40 ± 0.02	7.35 ± 0.02	7.32 ± 0.2

226

227 Table 1 caption:

228 Arterial blood gas levels were assessed in samples taken from conscious,
229 unrestrained mice chronically instrumented with femoral artery catheters at
230 baseline (room air) or during exposure to 6% inspired CO₂ or 7% O₂, 3.2% CO₂
231 to induce hypercapnia or isocapnic hypoxemia, respectively. No differences in
232 P_aO₂, P_aCO₂, or pH_a between paired WT and knockout groups were detected.
233 Values are means ± SE; n = 5-8 animals/group. *P < 0.05 vs. baseline (2-way,
234 repeated measures ANOVA; Sidak's post-hoc test).

235

236 First, we measured minute ventilation in mice exposed to 5 minutes of 3 levels of
237 inspired CO₂ (3.7, 6.0, and 9.8%) to determine an appropriate level for testing
238 hypercapnic ventilatory responses (Fig. 1A-D). In these pilot experiments, exposure to
239 3.7%, 6.0%, and 9.8% inspired CO₂ significantly elevated respiratory frequency (Fig.
240 1B), but only exposure to 6.0% and 9.8%, and not 3.7% inspired CO₂ caused
241 statistically significant elevations in tidal volume and minute ventilation (Fig. 1C and D,
242 respectively). We chose to use 6% CO₂ as the hypercapnic stimulus for the remaining
243 experiments in this study because it stimulated a robust response that was not
244 statistically different from the response caused by 9.8% CO₂. Using arterial blood
245 samples obtained via chronically implanted femoral artery catheters in conscious,
246 unrestrained WT mice, we assessed P_aO₂, P_aCO₂, and pH_a at baseline (room air) and
247 during exposure to 6% inspired CO₂. Although inspired O₂ was unchanged (21%) during
248 exposure to 6% inspired CO₂, P_aO₂ was increased (Fig. 1E) likely due to the resultant
249 increase in alveolar ventilation. As expected, mice exhibited hypercapnia and acidosis

250 indicated by increased $P_a\text{CO}_2$ and decreased pH_a during exposure to 6% inspired CO_2
251 (Figs. 1F and G).

252 Next, we measured $P_a\text{O}_2$, $P_a\text{CO}_2$, and pH_a in ASIC1^{-/-}, ASIC2^{-/-}, ASIC3^{-/-}, and
253 paired groups of WT mice. The purpose of this experiment was to determine if the
254 stimuli for ventilation ($P_a\text{O}_2$, $P_a\text{CO}_2$, and pH_a) were the same between WT and knockout
255 mice. Our results show no significant differences in $P_a\text{O}_2$, $P_a\text{CO}_2$, and pH_a between
256 ASIC1^{-/-}, ASIC2^{-/-}, or ASIC3^{-/-} versus corresponding WT mice at baseline or during
257 exposure to 6% inspired CO_2 (Table 1). To investigate the putative roles of ASIC1,
258 ASIC2, and ASIC3 in the hypercapnic/acidotic ventilatory response, we exposed
259 separate groups of ASIC1^{-/-}, ASIC2^{-/-}, and ASIC3^{-/-} mice to 6% inspired CO_2 and
260 measured respiratory frequency, tidal volume, and minute ventilation using whole-body
261 plethysmography as described above, and compared the responses to those of WT
262 mice run in parallel for each experiment. Surprisingly, there were no significant
263 differences between ASIC1^{-/-}, ASIC2^{-/-}, or ASIC3^{-/-} mice compared to WT mice in
264 respiratory frequency, tidal volume, or minute ventilation (Fig. 2). There was a tendency
265 for ASIC2^{-/-} mice to exhibit lower respiratory frequency during hypercapnia (Fig. 2D), but
266 this trend was not statistically significant ($p = 0.070$).

267

268 Figure 2 caption:

269 **The hypercapnic ventilatory response does not require ASIC1, 2, or**
270 **3.** Whole-body plethysmography was used to determine respiratory frequency
271 (breaths/min; A, D, G), tidal volume ($\mu\text{L}/\text{breath}/\text{g}$; B, E, H), and minute ventilation
272 ($\text{ml}/\text{min}/\text{g}$ body wt; C, F, I) at baseline and during exposure to hypercapnia (6%

273 CO₂) in WT, ASIC1^{-/-} (A-C), ASIC2^{-/-} (D-F), and ASIC3^{-/-} mice (G-I). Values are
274 means ± SE; n = 8 (A-C), 7-8 (D-F), or 11-12 (G-I) animals/group. **P* < 0.05 vs.
275 baseline (2-way, repeated measures ANOVA; Sidak's post-hoc test). Displayed *P*
276 value corresponds to comparison between WT and KO (panel D).

277

278 Assessing the roles of ASIC1, 2, and 3 in the hypoxic ventilatory response

279 To specifically assess the roles of ASICs in the ventilatory response to hypoxia,
280 we measured responses to isocapnic hypoxemia, which was achieved via inhalation of
281 a hypoxic gas mixture with a level of inspired CO₂ adequate to preserve baseline P_aCO₂
282 levels, allowing for the assessment of the hypoxic ventilatory response without
283 confounding changes in P_aCO₂/pH_a-dependent ventilatory drive. To determine the level
284 of inspired CO₂ required to achieve isocapnic hypoxemia, we measured baseline P_aCO₂
285 in WT animals, and then experimentally determined the level of inspired CO₂ necessary
286 to maintain this P_aCO₂ in mice concurrently exposed to 7% inspired O₂. Baseline P_aCO₂
287 in WT mice was 29.8 ± 0.9 mmHg. Mice chronically instrumented with femoral artery
288 catheters were exposed to 7% O₂ at a range of inspired CO₂ levels (2.5 - 3.5%) and the
289 resulting P_aCO₂ was assessed (Fig. 3A). Linear regression analysis of these data
290 indicate that an inspired CO₂ of 3.2% produces isocapnic hypoxemia. Testing this
291 exposure in a group of WT mice (n = 7) confirmed significant hypoxemia (Fig. 3B) with
292 no accompanying change in P_aCO₂ or pH_a (Figs. 3C-D). Whole-body plethysmography
293 measurements show that this exposure robustly increased respiratory frequency and
294 tidal volume (Fig. 3E). We used this stimulus (7% O₂, 3.2% CO₂, balance N₂) to
295 compare hypoxic ventilatory responses in the following experiments.

296

297 Figure 3 caption:

298 **An inspired CO₂ of 3.2% causes isocapnic hypoxemia in mice**
299 **concurrently exposed to 7.0% O₂.** A scatter plot **(A)** showing arterial CO₂
300 tensions (P_aCO₂; y-axis) in mice exposed to 7.0% O₂ and a range of inspired CO₂
301 levels (% CO₂; x-axis) was fit using linear regression (solid line, equation
302 displayed on the graph). The dotted lines on the graph indicate the average
303 baseline P_aCO₂ (horizontal) measured during exposure to room air, and the
304 estimated inspired CO₂ required to maintain this P_aCO₂ level (vertical) during
305 exposure to 7% O₂ based on the linear regression. Arterial blood samples from
306 WT mice exposed to 7.0% O₂, 3.2% CO₂, balance N₂, were analyzed to assess
307 P_aO₂ **(B)**, P_aCO₂ **(C)**, and pH_a **(D)**. **(E)** Representative whole-body
308 plethysmography traces from a WT mouse show the ventilatory response to
309 7.0% O₂, 3.2% CO₂, balance N₂. Values are individual measurements (A) or
310 means ± SE (B-D); n = 5-6 animals per group (B-D). **P* < 0.05 vs. baseline
311 (paired, two-tailed Student's t-test).

312

313 Using ASIC1^{-/-}, ASIC2^{-/-}, and ASIC3^{-/-}, and WT mice chronically instrumented
314 with femoral artery catheters, we measured P_aO₂, P_aCO₂, and pH_a to confirm that there
315 were no differences in blood gases between respective knockout and WT mice at
316 baseline or during exposure to 7% O₂, 3.2% CO₂, balance N₂ (Table 1), demonstrating
317 that a similar hypoxic stimulus was achieved between groups. Although a slight but
318 significant decrease in P_aCO₂ occurred in response to this inspired gas mixture

319 compared to baseline in some groups (marked with asterisks, Table 1), in all cases
320 there were no significant differences between paired WT and knockout groups. To test
321 the roles of ASIC1, 2, and 3 in the hypoxic ventilatory response, separate groups of
322 conscious, unrestrained ASIC1^{-/-}, ASIC2^{-/-}, ASIC3^{-/-}, and WT mice were exposed to 7%
323 O₂, 3.2% CO₂, balance N₂ to induce isocapnic hypoxemia and their respiratory
324 frequencies, tidal volumes, and minute ventilations were assessed using whole-body
325 plethysmography (Fig. 4). There were no differences in ventilatory parameters between
326 ASIC1^{-/-} or ASIC3^{-/-} and WT mice (Fig. 4A-C, G-I). ASIC2^{-/-} mice tended to have lower
327 respiratory frequency and tidal volume than WT mice during exposure to isocapnic
328 hypoxemia (Fig. 4D, E). While these trends in respiratory frequency and tidal volume
329 were not statistically significant, minute ventilation was significantly lower in ASIC2^{-/-}
330 mice compared to WT (Fig. 4F), suggesting a role for ASIC2 in the hypoxic ventilatory
331 response.

332

333 Figure 4 caption:

334 **ASIC2, but not ASIC1 or ASIC3, contributes to the hypoxic**
335 **ventilatory response.** Ventilatory responses to isocapnic hypoxemia (7.0% O₂,
336 3.2% CO₂, bal N₂) were assessed using whole-body plethysmography and
337 compared between **(A-C)** ASIC1^{-/-}, **(D-F)** ASIC2^{-/-}, and **(G-I)** ASIC3^{-/-} and WT
338 mice. Values are means ± SE; n = 8 (A-F) or 11-12 (G-I) animals/group. **P* <
339 0.05 vs. baseline; #*P* < 0.05 vs. WT (2-way, repeated measures ANOVA; Sidak's
340 post-hoc test). Displayed *P* value corresponds to the comparison between WT
341 and KO (panel D).

342

343 Discussion

344 Previous evidence indicates that ASICs are involved in chemoreception and the
345 control of ventilation (16–19,23,24), but most of this evidence comes from *in vitro*
346 studies and little is known about the role of ASICs in hypercapnic and hypoxic
347 ventilatory responses in conscious animals. Here we directly measured hypercapnic
348 and hypoxic ventilatory responses in conscious, unrestrained mice. In contrast to our
349 hypothesis, we found that genetic deletion of ASIC1, 2, or 3 does not alter the
350 hypercapnic ventilatory response in mice; whereas ASIC2 appears to play a minor role
351 in the hypoxic ventilatory response. Together, these data suggest the contribution of
352 ASICs to ventilatory control is modest.

353 ASICs have been implicated in both peripheral and central CO₂ chemoreception.
354 Isolated carotid body glomus type I cells exhibit acid (pH 6.0-6.8)-induced cation
355 currents and depolarization which have been attributed to ASICs (16). Further
356 investigation revealed that pH-sensitivity in isolated glomus cells is increased in both
357 transgenic ASIC3 overexpressing mice and spontaneously hypertensive rats with
358 increased expression of ASIC3, and decreased in ASIC3 null mice (23,24). These
359 studies suggest that ASIC3 would contribute to hypercapnic ventilatory drive. However,
360 the pH levels used to stimulate a response in these *in vitro* experiments ranged from pH
361 6.0 to 6.8. In the present study, exposure to 6% inspired CO₂ caused a 70% increase in
362 P_aCO₂, resulting in a pH_a of 7.2. This stimulus caused a robust ventilatory response
363 (Figs. 1, 2), yet a pH_a of 7.2 may be insufficient to activate ASICs.

364 Other reports implicate ASICs in *central* chemoreception. The response of
365 central chemoreceptors to changes in pH is known to be very sensitive, in that changes

366 in cerebrospinal fluid pH from 7.30 to 7.25 cause a doubling in alveolar ventilation (25).
367 In neurons of the nucleus tractus solitarius in brainstem slices, acidification to pH 7.0
368 causes transient inward currents that are blocked by amiloride (18). Although amiloride
369 is a non-selective blocker of ASICs, Song et al., found that the selective ASIC1a
370 blocker, psalmotoxin-1 (PcTX1) inhibited the increased phrenic nerve discharge in
371 response to injection of acidified (pH 6.5) artificial cerebrospinal fluid in the lateral
372 hypothalamus (17). Furthermore, these authors report ASIC-like acid-induced currents
373 in the ventrolateral medulla were absent in ASIC1^{-/-} mice (19). These data provide
374 strong evidence that ASIC1 contributes to central chemoreception in response to direct
375 changes in pH (pH 6.0 – 7.0), however whether the observed effect is relevant to the
376 physiological ventilatory response to hypercapnia is less clear. The threshold for
377 activation of ASIC1 and ASIC3 is ~ pH 7.0 - 7.2 (26,27) and the half-maximal activation
378 is 6.2 - 6.8 for ASIC1a, ~4.9 for ASIC2a, and 6.5 - 6.7 for ASIC3 (26,28). Interestingly,
379 however, Ziemann et al. reported that inhalation of higher CO₂ concentrations (10 and
380 20%) in anesthetized mice leads to a drop in pH ranging from 6.7- 6.9 in the amygdala
381 and lateral ventricle (29). Consistent with our findings, the authors demonstrated an
382 intact ventilatory response to CO₂ inhalation (5 and 10%) in ASIC1^{-/-} mice despite the
383 important chemosensory role ASIC1 plays in the amygdala and fear-related behavior
384 (29). Acid-evoked ASIC responses in isolated cells tend to be transient, on the order of
385 seconds, while the ventilatory response to hypercapnia is sustained indefinitely. This
386 might explain why the previously reported contribution of ASIC3 to transient acid-
387 induced currents in isolated glomus cells (16,24) does not translate to a contribution to
388 the hypercapnic ventilatory response. However, the studies implicating ASICs in central

389 chemoreception reported sustained changes to phrenic nerve discharge (17–19),
390 suggesting that ASICs can mediate sustained responses to extracellular acidification in
391 some contexts.

392 Thus, despite strong evidence for ASICs in chemoreception, our current findings
393 do not support a role for ASICs in the hypercapnic ventilatory response in conscious,
394 unrestrained mice. Although differences in ventilatory regulation may exist between
395 species, mice are widely used in ventilatory function studies as they show dependency
396 both on carotid bodies (30) as well as central chemoreception (1) for control of
397 ventilation. Furthermore, mice were used to study the involvement of ASICs in carotid
398 body glomus cells (24) and central chemoreception (19). Therefore, it is unlikely that
399 our current findings are due to species differences in control of ventilation. Inhalation of
400 6% CO₂ was chosen as the stimulus for hypercapnic ventilatory responses based on
401 the preliminary data presented in figure 1 which indicates that 6% CO₂ causes a near-
402 maximal ventilatory response. Although we cannot exclude the potential for ASICs to
403 participate in hypercapnic ventilatory responses to higher levels of CO₂, this seems
404 unlikely since the response of WT mice to 9.7% CO₂ was not different compared to the
405 response to 6% CO₂. Additionally, our results agree with the findings of Ziemann et al.
406 (29) which indicated that ASIC1 was not involved in ventilatory responses to 5% or 10%
407 inspired CO₂.

408 Although much of the evidence supporting ASIC involvement in chemoreception
409 focuses on the detection and ventilatory response to CO₂ or acidosis, evidence
410 suggests ASICs may also be hypoxia-sensitive. For example, we have previously
411 reported that ASIC1 contributes to HPV in isolated-perfused lungs (20). Additionally,

412 activation of the Ca²⁺-permeable ASIC1a **contributes to neuronal cell death during**
413 **ischemic brain injury** (31,32). Currently however, it is unclear whether the **activation of**
414 **ASICs responsible for neuronal cell death in this context results from** the associated
415 acidosis, or a direct effect of hypoxia. Liu et al reported that the hypoxia-induced
416 chemoreceptor response and ASIC expression are both increased following exposure to
417 *chronic* hypobaric hypoxia (380 Torr ambient air pressure for 1-7 days) in the rat
418 petrosal ganglion, which contains chemoafferent neurons that innervate O₂-sensitive
419 carotid body glomus type I cells (33). Pharmacological inhibition of ASICs using A-
420 317576 (novel ASIC blocker (34)) or ibuprofen (non-specific ASIC inhibitor (35))
421 prevented the enhanced hypoxia-evoked chemoreceptor response following exposure
422 of rats to chronic hypoxia, but did not alter the hypoxic chemoreceptor response in
423 normoxia-exposed control animals (33). In contrast, Lu et al. demonstrated that
424 transgenic overexpression of ASIC3 leads to decreased glomus cell sensitivity to
425 sodium cyanide (used to mimic hypoxia) (24). Together, these data are consistent with
426 the hypothesis that ASICs modulates hypoxic chemotransmission between type I cells
427 and chemoafferent neurons. In the present study, we have differentiated between
428 hypoxia and acidosis by utilizing *isocapnic* hypoxemia as a ventilatory stimulus that
429 maintains baseline CO₂ and pH levels. Ventilatory responses to isocapnic hypoxemia
430 were normal in ASIC1^{-/-} and ASIC3^{-/-} mice, but reduced in ASIC2^{-/-} mice (Fig. 4F)
431 suggesting a minor role for ASIC2 in this response. **ASIC2a was reported to be**
432 **expressed in carotid body glomus cells (16), and may contribute to the hypoxic**
433 **ventilatory response by contributing to the depolarization of these cells during**
434 **hypoxemia.**

435 In summary, our data bring into question the physiological relevance of ASICs in
436 chemoreception and the control of ventilation. We cannot rule out the possibility that
437 compensatory upregulation of parallel chemoreception and ventilatory control pathways
438 masks any effect of ASIC deletion in our global knockout mice. Furthermore, cerebral
439 ischemia or other pathophysiological conditions might unmask a contribution of ASICs
440 to hypercapnic and/or hypoxic ventilatory drive. Because ASICs are potential
441 therapeutic targets for the treatment of pulmonary hypertension (20) and several
442 neuronal diseases (36), a complete understanding of the roles ASICs play in O₂ and
443 CO₂ homeostasis is important to the development of safe therapeutics.

444 **Acknowledgements:**

445 We thank Anthony Gravagne in the Department of Physics and Astronomy at the
446 University of New Mexico for his assistance with the design and fabrication of the
447 plethysmography chamber. We also thank Lindsay Herbert for her assistance with
448 knockout mouse colony maintenance.

449 **References:**

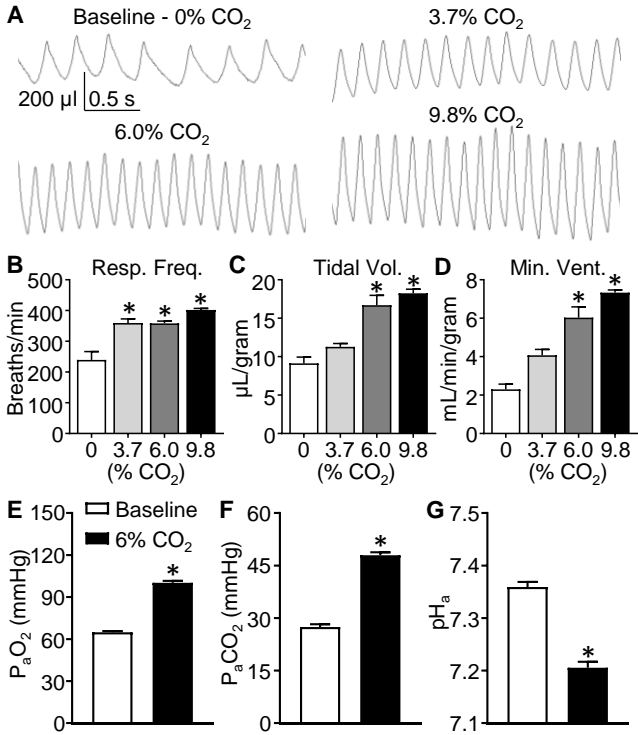
- 450 1. Nattie E, Li A. Central chemoreceptors: Locations and functions. *Compr Physiol.*
451 2012;2(1):221–54.
- 452 2. Buckler KJ. A novel oxygen-sensitive potassium current in rat carotid body type I
453 cells. *J Physiol.* 1997 Feb 1;498(3):649–62.
- 454 3. Delpiano MA, Hescheler J. Evidence for a PO₂ -sensitive K⁺ channel in the type-I
455 cell of the rabbit carotid body. *FEBS Lett.* 1989 Jun 5;249(2):195–8.
- 456 4. Kim D, Cavanaugh EJ, Kim I, Carroll JL. Heteromeric TASK-1/TASK-3 is the
457 major oxygen-sensitive background K⁺ channel in rat carotid body glomus cells. *J*
458 *Physiol.* 2009 Jun 15;587(12):2963–75.
- 459 5. López-López JR, Pérez-García MT. Oxygen sensitive Kv channels in the carotid
460 body. *Respir Physiol Neurobiol.* 2007 Jul;157(1):65–74.
- 461 6. Ureña J, Fernández-Chacón R, Benot AR, Alvarez de Toledo GA, López-Barneo
462 J. Hypoxia induces voltage-dependent Ca²⁺ entry and quantal dopamine
463 secretion in carotid body glomus cells. *Proc Natl Acad Sci U S A.* 1994 Oct
464 11;91(21):10208–11.
- 465 7. Ortega-Sáenz P, Levitsky KL, Marcos-Almaraz MT, Bonilla-Henao V, Pascual A,
466 López-Barneo J. Carotid body chemosensory responses in mice deficient of
467 TASK channels. *J Gen Physiol.* 2010 Apr;135(4):379–92.
- 468 8. Peers C. Hypoxic suppression of K⁺ currents in type I carotid body cells: Selective
469 effect on the Ca²⁺-activated K⁺ current. *Neurosci Lett.* 1990 Nov;119(2):253–6.
- 470 9. Guyenet PG, Stornetta RL, Bayliss DA. Central respiratory chemoreception. *J*
471 *Comp Neurol.* 2010 May 20;518(19):3883–906.

- 472 10. Bayliss DA, Talley EM, Sirois JE, Lei Q. TASK-1 is a highly modulated pH-
473 sensitive “leak” K⁺ channel expressed in brainstem respiratory neurons. *Respir*
474 *Physiol.* 2001 Dec;129(1–2):159–74.
- 475 11. Mulkey DK, Talley EM, Stornetta RL, Siegel AR, West GH, Chen X, et al. TASK
476 Channels Determine pH Sensitivity in Select Respiratory Neurons But Do Not
477 Contribute to Central Respiratory Chemosensitivity. *J Neurosci.* 2007 Dec
478 19;27(51):14049–58.
- 479 12. Wang S, Benamer N, Zanella S, Kumar NN, Shi Y, Bevengut M, et al. TASK-2
480 Channels Contribute to pH Sensitivity of Retrotrapezoid Nucleus Chemoreceptor
481 Neurons. *J Neurosci.* 2013 Oct 9;33(41):16033–44.
- 482 13. Gestreau C, Heitzmann D, Thomas J, Dubreuil V, Bandulik S, Reichold M, et al.
483 Task2 potassium channels set central respiratory CO₂ and O₂ sensitivity. *Proc*
484 *Natl Acad Sci.* 2010 Feb 2;107(5):2325–30.
- 485 14. Price MP, Lewin GR, McIlwrath SL, Cheng C, Xie J, Heppenstall PA, et al. The
486 mammalian sodium channel BNC1 is required for normal touch sensation. *Nature.*
487 2000 Oct 26;407(6807):1007–11.
- 488 15. Bartoi T, Augustinowski K, Polleichtner G, Grunder S, Ulbrich MH. Acid-sensing
489 ion channel (ASIC) 1a/2a heteromers have a flexible 2:1/1:2 stoichiometry. *Proc*
490 *Natl Acad Sci.* 2014 Jun 3;111(22):8281–6.
- 491 16. Tan ZY, Lu Y, Whiteis CA, Benson CJ, Chapleau MW, Abboud FM. Acid-sensing
492 ion channels contribute to transduction of extracellular acidosis in rat carotid body
493 glomus cells. *Circ Res.* 2007;101(10):1009–19.
- 494 17. Song N, Zhang G, Geng W, Liu Z, Jin W, Li L, et al. Acid sensing ion channel 1 in

- 495 lateral hypothalamus contributes to breathing control. *PLoS One*. 2012;7(7):1–10.
- 496 18. Huda R, Pollema-Mays SL, Chang Z, Alheid GF, McCrimmon DR, Martina M.
497 Acid-sensing ion channels contribute to chemosensitivity of breathing-related
498 neurons of the nucleus of the solitary tract. *J Physiol*. 2012;590(Pt 19):4761–75.
- 499 19. Song N, Guan R, Jiang Q, Hassanzadeh CJ, Chu Y, Zhao X, et al. Acid-sensing
500 ion channels are expressed in the ventrolateral medulla and contribute to central
501 chemoreception. *Sci Rep*. 2016;6(December):38777.
- 502 20. Nitta CH, Osmond DA, Herbert LM, Beasley BF, Resta TC, Walker BR, et al. Role
503 of ASIC1 in the development of chronic hypoxia-induced pulmonary hypertension.
504 *AJP Hear Circ Physiol*. 2014 Jan 1;306(1):H41–52.
- 505 21. Drorbaugh JE, Fenn WO. A barometric method for measuring ventilation in
506 newborn infants. *Pediatrics*. 1955 Jul;16(1):81–7.
- 507 22. Walker BR, Adams EM, Voelkel NF. Ventilatory responses of hamsters and rats
508 to hypoxia and hypercapnia. *J Appl Physiol*. 1985 Dec;59(6):1955–60.
- 509 23. Tan ZY, Lu Y, Whiteis CA, Simms AE, Paton JFR, Chapleau MW, et al.
510 Chemoreceptor hypersensitivity, sympathetic excitation, and overexpression of
511 ASIC and TASK channels before the onset of hypertension in SHR. *Circ Res*.
512 2010;106(3):536–45.
- 513 24. Lu Y, Whiteis C a, Sluka K a, Chapleau MW, Abboud FM. Responses of glomus
514 cells to hypoxia and acidosis are uncoupled, reciprocal and linked to ASIC3
515 expression: selectivity of chemosensory transduction. *J Physiol*. 2013;591(Pt
516 4):919–32.
- 517 25. Fencel V, Miller TB, Pappenheimer JR. Studies on the respiratory response to

- 518 disturbances of acid-base balance, with deductions concerning the ionic
519 composition of cerebral interstitial fluid. *Am J Physiol.* 1966;210(3):459–72.
- 520 26. Kress M, Waldmann R. Chapter 8 Acid Sensing Ionic Channels. In 2006. p. 241–
521 76.
- 522 27. Wemmie JA, Price MP, Welsh MJ. Acid-sensing ion channels: advances,
523 questions and therapeutic opportunities. *Trends Neurosci.* 2006 Oct;29(10):578–
524 86.
- 525 28. Benson CJ, Xie J, Wemmie JA, Price MP, Henss JM, Welsh MJ, et al.
526 Heteromultimers of DEG/ENaC subunits form H⁺-gated channels in mouse
527 sensory neurons. *Proc Natl Acad Sci U S A.* 2002 Feb 19;99(4):2338–43.
- 528 29. Ziemann AE, Allen JE, Dahdaleh NS, Drebot II, Coryell MW, Wunsch AM, et al.
529 The Amygdala Is a Chemosensor that Detects Carbon Dioxide and Acidosis to
530 Elicit Fear Behavior. *Cell.* 2009;139(5):1012–21.
- 531 30. Izumizaki M. Role of the carotid bodies in chemosensory ventilatory responses in
532 the anesthetized mouse. *J Appl Physiol.* 2004 May 14;97(4):1401–7.
- 533 31. Xiong ZG, Xu T Le. The role of ASICs in cerebral ischemia. *Wiley Interdiscip Rev*
534 *Membr Transp Signal.* 2012;1(5):655–62.
- 535 32. Xiong ZG, Zhu XM, Chu XP, Minami M, Hey J, Wei WL, et al. Neuroprotection in
536 ischemia: Blocking calcium-permeable acid-sensing ion channels. *Cell.*
537 2004;118(6):687–98.
- 538 33. Liu X, He L, Dinger B, Fidone SJ. Chronic hypoxia-induced acid-sensitive ion
539 channel expression in chemoafferent neurons contributes to chemoreceptor
540 hypersensitivity. *AJP Lung Cell Mol Physiol.* 2011;301(6):L985–92.

- 541 34. Dubé GR, Lehto SG, Breese NM, Baker SJ, Wang X, Matulenko MA, et al.
542 Electrophysiological and in vivo characterization of A-317567, a novel blocker of
543 acid sensing ion channels. *Pain*. 2005 Sep;117(1):88–96.
- 544 35. Voilley N, de Weille J, Mamet J, Lazdunski M. Nonsteroid anti-inflammatory drugs
545 inhibit both the activity and the inflammation-induced expression of acid-sensing
546 ion channels in nociceptors. *J Neurosci*. 2001 Oct 15;21(20):8026–33.
- 547 36. Wemmie JA, Taugher RJ, Kreple CJ. Acid-sensing ion channels in pain and
548 disease. *Nat Rev Neurosci*. 2013 Jun 20;14(7):461–71.
- 549



Single column width

Fig. 1

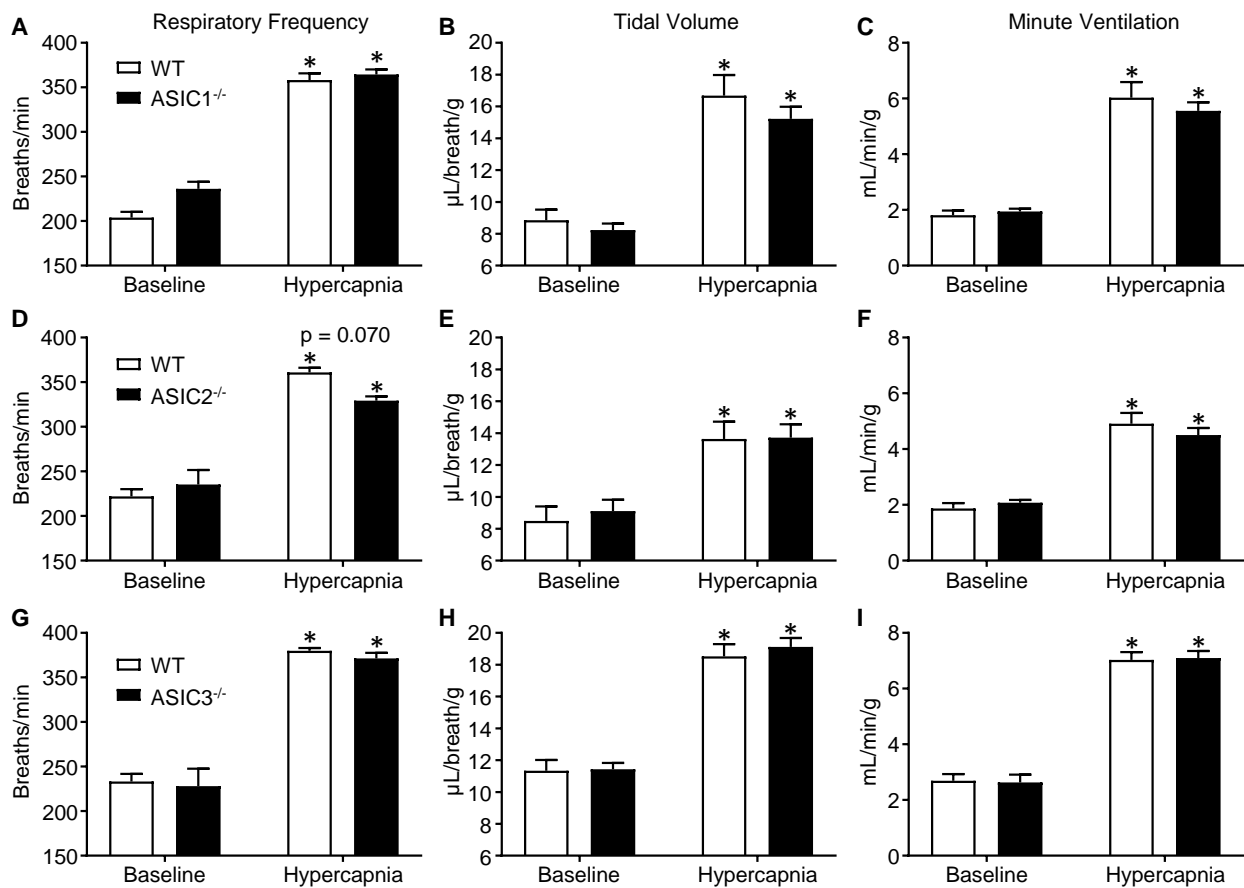
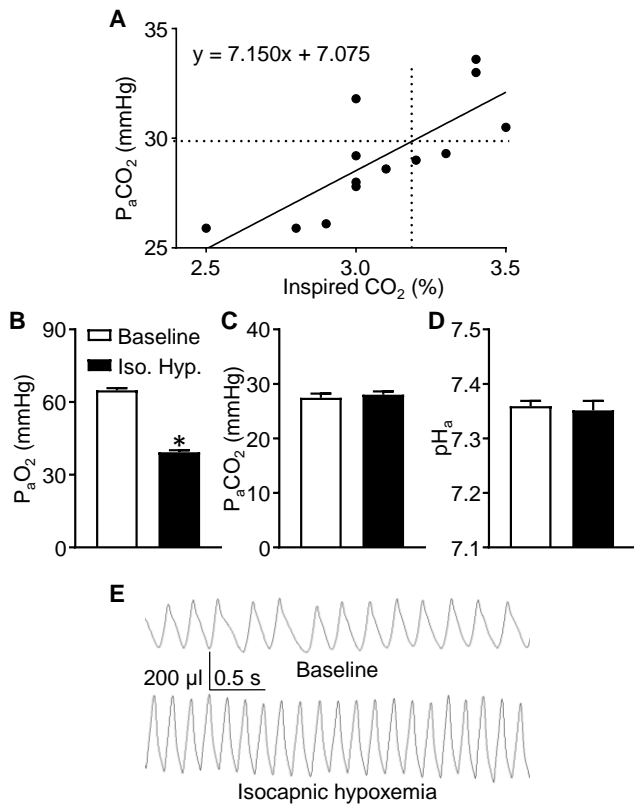


Fig. 2



Single column width

Fig. 3

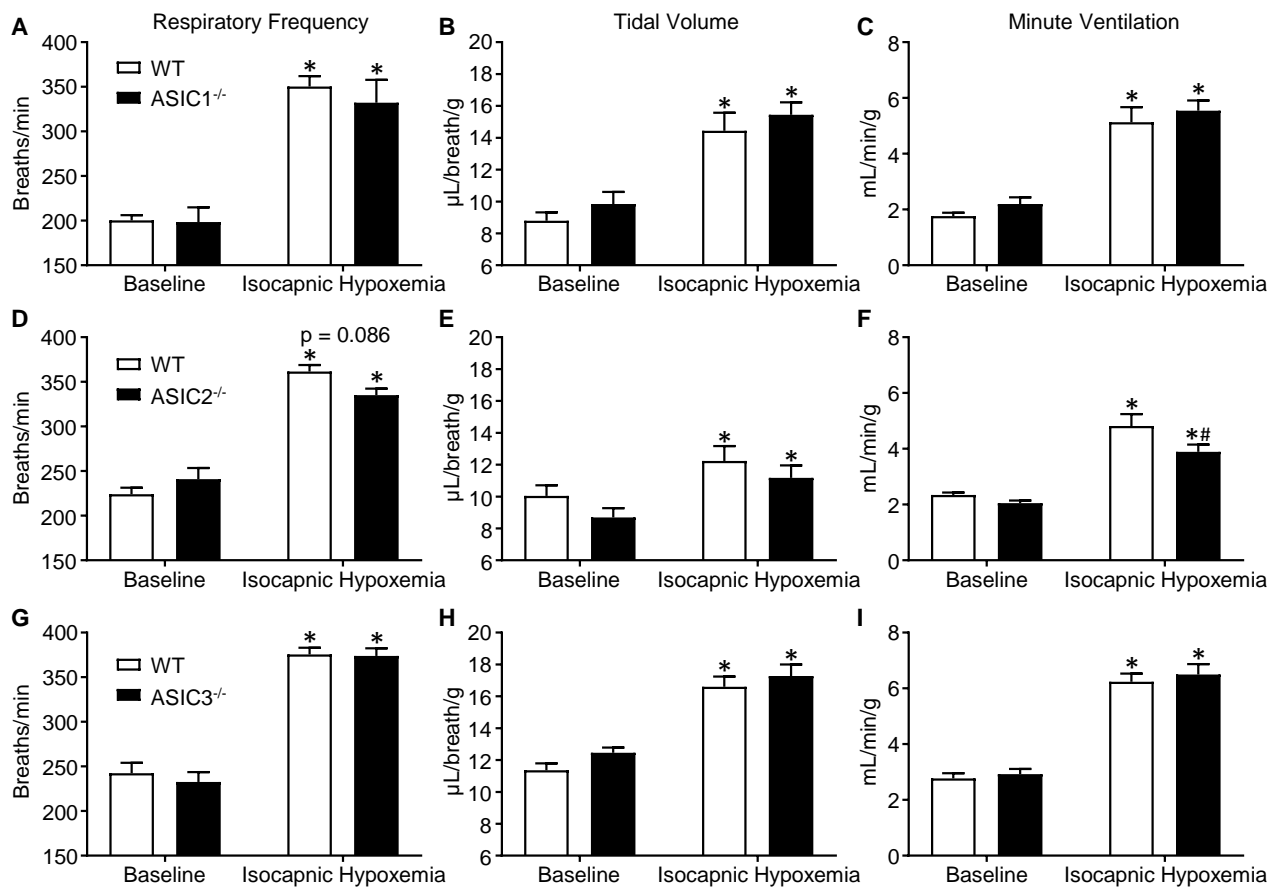


Fig. 4